ELSEVIER

Nuclear Instruments and Methods in Physics Research B 154 (1999) 32–40

NIM B
Beam Interactions with Materials & Atoms

www.elsevier.nl/locate/nimb

Multivariable hypergeometric functions for ion–atom collisions

G. Gasaneo [a,*], F.D. Colavecchia [b], C.R. Garibotti [b]

[a] *Universidad Nacional del Sur, 8000 Bahía Blanca, Buenos Aires, Argentina*
[b] *Centro Atómico Bariloche, 8400 S.C. de Bariloche, Río Negro, Argentina*

Abstract

In this work we present a correlated wave function for a three-body continuum Coulomb problem. This state is described by the two-variables Φ_2 hypergeometric function. We examine the properties of this function and their differences with previous uncorrelated models. The Φ_2 wave function can be considered as a final state of ion–atom ionizing collisions, giving rise to both undistorted (Born-Φ_2) and distorted (EIS-Φ_2) models. We obtain double differential cross sections with the Born-Φ_2 theory for proton–helium collisions in the intermediate to high energy regime. They exhibit all the main features of the electronic emission process and agree with the experimental data.

PACS: 34.50.Fa; 03.65.Nk; 02.70.Rw
Keywords: Three-body problem; Collisional ionization

1. Introduction

Three main characteristics arise in the ejected electron spectra in ionizing ion–atom collisions: the soft electron peak (SE), a structure in the region where the electrons are ejected with small velocities relative to the target; the electron capture to the continuum (ECC) state of the projectile given by a sharp peak centered at the projectile velocity and the binary sphere (BE), a smooth structure where the electrons would lie after a head-on collision with the projectile. An enhancement of the electronic emission with velocities between zero and the projectile velocity (ridge electrons) connects the SE and ECC peaks. While these structures have been very well studied along the years, many questions are still unsolved. Some kinematically complete experiments have been carried out [1], but double differential cross sections (DDCS) in the forward direction for the simple proton-atomic hydrogen collision have not been measured yet. There are many theoretical approaches to the ionization problem, but they are accurate for some impact energies and regions of the spectra of emitted electrons [2]. Furthermore, these theoretical models give only a rough approach to the dynamic of the three-body Coulomb problem. The main shortcoming of these theories is that they do not explicitly include the correlation between the motion of the electron relative to the target and the projectile. For

* Corresponding author. E-mail: ggasaneo@criba.edu.ar.

0168-583X/99/$ – see front matter
PII: S0168-583X(99)00186-X

example, the multiple scattering [3], the continuum distorted wave [4–6] and the impulse approximation [7] have a common representation of the final channel when the electron is in the continuum of both the target and projectile. This final state is the well known C3 function [3], where all interactions are taken independently, resulting in a product of three two-body Coulomb wave function. Recently, some modified functions have been proposed that take into account some asymptotic properties when two particles are close to each other and far from the third [8–11]. However, calculation of DDCS with these functions is numerically difficult and does not seem to improve the agreement with experimental data. Hence it is clear that a more comprehensive theory is necessary to obtain a complete description of the ionization process.

In this work we present a theory based on a correlated approximate solution of the three-body continuum Coulomb problem. This solution can be written as the multivariable hypergeometric function Φ_2 of Erdelyi [12,13]. In Section 2 we describe the properties of the Φ_2 wave function and the possible extensions of this approach. In Section 3 we develop the undistorted and distorted versions of the theory and describe some features of the DDCS obtained with these models. Finally, we discuss some perspectives of this theory in Section 4. Atomic units are used unless otherwise is noted.

2. The correlated model Φ_2

The C3 approach is a non-correlated wave function which has been used to represent the motion of three charged particles when the total energy of the system is greater than the total break-up [3]. It does not consider coupling between the three two-body subsystems. We remove the energy $E = k_t^2/2\mu_t + K_t^2/2v_t$ replacing the ansatz

$$\overline{\Psi}(\mathbf{r}_t, \mathbf{R}_t) = \exp(\mathrm{i}\mathbf{k}_t \cdot \mathbf{r}_t + \mathrm{i}\mathbf{K}_t \cdot \mathbf{R}_t)\Psi(\mathbf{r}_t, \mathbf{R}_t)$$

in the time-independent Schrödinger equation $[H - E]\overline{\Psi} = 0$ and then write the resulting equation in terms of the parabolic coordinates introduced by Klar [14]

$$\xi_i = r_i + \hat{\mathbf{k}}_i \cdot \mathbf{r}_i, \quad \eta_i = r_i - \hat{\mathbf{k}}_i \cdot \mathbf{r}_i, \quad i \in \{t, p, tp\}.$$

The momenta $\mathbf{K}_t$ and $\mathbf{k}_t$ form a Jacobi pair, and $\mathbf{r}_i$ and $\mathbf{k}_i$ ($i \in \{t, p, tp\}$ are the relative coordinate and momenta between pairs of particles (we follow the notation of Ref. [15]). The equation that governs the dynamics of the system is

$$[D_0 + D_1 + V]\Psi = 0, \tag{1}$$

where

$$D_0 = H_t + H_p + H_{tp}, \tag{2}$$

$$D_1 = \frac{1}{m_e} W_t\, W_p + \frac{1}{m_t} W_t\, W_{tp} - \frac{1}{m_p} W_p\, W_{tp}, \tag{3}$$

$$V = V_t + V_p + V_{tp} \tag{4}$$

and $V_t = Z_e Z_t / r_t$, $V_p = Z_e Z_p / r_p$ and $V_{tp} = Z_t Z_p / r_{tp}$ are the Coulomb potentials due to the charges Z_e, Z_t and Z_p, and the operators H_j and W_j are given by

$$H_j = \frac{1}{\mu_j r_j}\left[\xi_j \frac{\partial^2}{\partial \xi_j^2} + \left(1 + \mathrm{i}k_j\xi_j\right)\frac{\partial}{\partial \xi_j} + \eta_j \frac{\partial^2}{\partial \eta_j^2} + \left(1 - \mathrm{i}k_j\eta_j\right)\frac{\partial}{\partial \eta_j}\right], \qquad j \in \{t, p, tp\}, \tag{5}$$

$$W_j = \left(\hat{\mathbf{r}}_j + \hat{\mathbf{k}}_j\right)\frac{\partial}{\partial \xi_j} + \left(\hat{\mathbf{r}}_j - \hat{\mathbf{k}}_j\right)\frac{\partial}{\partial \eta_j}, \quad j \in \{t, p, tp\}. \tag{6}$$

For the case of two heavy (m_t and m_p) and a light (m_e) particles, D_1 could be approximated by the first term in Eq. (3). The solution of the general Eq. (1) or that resulting after the masses simplifications is unknown at present. Nevertheless, by considering the operator D_1 in an approximated way it is possible to obtain a function which correlates the motion of the small particle with the heavy ones. We introduce the following approximation:

$$D_1 \simeq \frac{1}{m_e}\left[\left(\frac{\xi_t}{r_p} + \frac{\xi_p}{r_t}\right)\frac{\partial^2}{\partial \xi_t \partial \xi_p} + \left(\frac{\eta_t}{r_p} + \frac{\eta_p}{r_t}\right)\frac{\partial^2}{\partial \eta_t \partial \eta_p} + \left(\frac{\xi_t}{r_p} + \frac{\eta_p}{r_t}\right)\frac{\partial^2}{\partial \xi_t \partial \eta_p} + \left(\frac{\eta_t}{r_p} + \frac{\xi_p}{r_t}\right)\frac{\partial^2}{\partial \eta_t \partial \xi_p}\right], \tag{7}$$

and furthermore assume solutions depending on ξ_i only, that give outgoing waves. Solving the equation which results replacing Eq. (7) in Eq. (1) we get the approximated three-body solution $\Psi_{\Phi_2}(\mathbf{r}_t,\mathbf{R}_t)$ [16,17]

$$\Psi_{\Phi_2}(\mathbf{r}_t,\mathbf{R}_t) = {}_1F_1\big[-\mathrm{i}\alpha_{tp},1,-\mathrm{i}k_{tp}\xi_{tp}\big]\times\Psi_f^{\Phi_2}(\mathbf{r}_t,\mathbf{R}_t), \tag{8}$$

$$\Psi_f^{\Phi_2}(\mathbf{r}_t,\mathbf{R}_t) = N\exp(\mathrm{i}\mathbf{k}_t\cdot\mathbf{r}_t+\mathrm{i}\mathbf{K}_t\cdot\mathbf{R}_t) \times\Phi_2\big[-\mathrm{i}\alpha_t,-\mathrm{i}\alpha_p,1,-\mathrm{i}k_t\xi_t,-\mathrm{i}k_p\xi_p\big],$$

where ${}_1F_1[b,c,z]$ is the confluent hypergeometric function [18]. The $\Phi_2[\beta,\beta',\gamma,x,y]$ is a generalized confluent hypergeometric function of two variables [19], α_i are the Sommerfeld parameter i.e. $\alpha_t=\mu_t Z_t Z_e/k_t$ and the normalization constant N to unit outgoing flux is given by

$$N = N_{tp}N_{\Phi_2} = \big[\mathrm{e}^{\pi/2\alpha_{tp}}\Gamma(1-\mathrm{i}\alpha_{tp})\big]\Big[\mathrm{e}^{\pi/2(\alpha_t+\alpha_p)}\Gamma(1-\mathrm{i}\alpha_t-\mathrm{i}\alpha_p)\Big], \tag{9}$$

with $\Gamma(x)$ the gamma function. The wave function given by Eq. (8) satisfies the Redmond asymptotic conditions [20]. Another useful expression for $\Psi_{\Phi_2}(\mathbf{r}_t,\mathbf{R}_t)$ is [21]

$$\Psi_{\Phi_2}(\mathbf{r}_t,\mathbf{R}_t) = N\exp(\mathrm{i}\mathbf{k}_t\cdot\mathbf{r}_t+\mathrm{i}\mathbf{K}_t\cdot\mathbf{R}_t)\ {}_1F_1\big[-\mathrm{i}\alpha_{tp},1,-\mathrm{i}k_{tp}\xi_{tp}\big] \times\sum_{m=0}^{\infty}a_m F_t[m,\xi_t]F_p\big[m,\xi_p\big], \tag{10}$$

where

$$F_j\big[m,\xi_j\big] = \big(-k_j\xi_j\big)^m {}_1F_1\big[-\mathrm{i}\alpha_j+m,1+2m,-\mathrm{i}k_j\xi_j\big],\quad j\in\{t,p\}, \tag{11}$$

$$a_m = \frac{(-\mathrm{i}\alpha_t)_m(-\mathrm{i}\alpha_p)_m}{m!(m)_m(1)_{2m}}, \tag{12}$$

and $(a)_m$ is the Pochhammer symbol. In Eq. (10), the Φ_2 function is written as a series expansion in terms of the solutions of two-dimensional oscillators [22]. We would like to note that each product $F_t[m,\xi_t]F_p\big[m,\xi_p\big]$ satisfies the correct asymptotic conditions in the region where all particles are far from each other and can be considered itself as a final wave function for an ionization process. A natural generalization of function $\Psi_f^{\Phi_2}$ can be constructed upon a sum over all of these product states with different coefficients a_m. The first term of Eq. (10) is, besides of the normalization constant, the non-correlated C3 wave

$$\Psi_{C3}(\mathbf{r}_t,\mathbf{R}_t) = N_{C3}\exp(\mathrm{i}\mathbf{k}_t\cdot\mathbf{r}_t+\mathrm{i}\mathbf{K}_t\cdot\mathbf{R}_t) \times{}_1F_1\big[-\mathrm{i}\alpha_t,1,-\mathrm{i}k_t\xi_t\big] \times{}_1F_1\big[-\mathrm{i}\alpha_p,1,-\mathrm{i}k_{tp}\xi_p\big] \times{}_1F_1\big[-\mathrm{i}\alpha_{tp},1,-\mathrm{i}k_{tp}\xi_{tp}\big], \tag{13}$$

$$N_{C3} = \mathrm{e}^{\frac{\pi}{2}(\alpha_t+\alpha_p+\alpha_{tp})}\Gamma(1-\mathrm{i}\alpha_t)\Gamma\big(1-\mathrm{i}\alpha_p\big)\Gamma\big(1-\mathrm{i}\alpha_{tp}\big). \tag{14}$$

It is also possible to obtain other correlated solutions depending on different parabolic coordinates using the approximation (7), these function will have different asymptotic behavior in the Ω_0 region [8,14,22].

In the C3 model the normalization is given by a superposition of three two-body normalizations $\mathrm{e}^{\pi/2\alpha_i}\Gamma(1-\mathrm{i}\alpha_i)$. Meanwhile, in the Φ_2 model, the associate normalization is correlated. As we can see, N_{Φ_2} include both Sommerfeld parameters in a single non-separable Gamma function. In Fig. 1 we show the square modulus of N_{C3} and N as a function of k_t for $K_t=2$ a.u., $Z_t=Z_p=1$ and $Z_e=-1$. The picture shows that the normalization N is more symmetrical than N_{C3}. As we shall see Section 3, the Φ_2 model gives a contribution to the asymmetry of the ECC peak larger than in the C3, we should look for the reason of this behavior in the whole wave function. When the charge Z_t or Z_p becomes large or k_{tp} becomes small both N and N_{C3} give rise to equivalent exclusion hole, produced by the repulsion between the charges of the same sign. We note that in the present approach the repulsive interaction remains uncorrelated, as in the C3 wave model.

A plot of the different orders of $\Psi_f^{\Phi_2}(\mathbf{r}_t,\mathbf{R}_t)$ as was defined by Eq. (10) leads us to understand how the correlation appears. We plot a particle distribution defined by the square modulus of $\Psi_{\Phi_2}(\mathbf{r}_t,\mathbf{R}_t)$ in terms of the parabolic coordinates, using the same charges and momenta as in Fig. 1. In this way we get a particle distribution of an

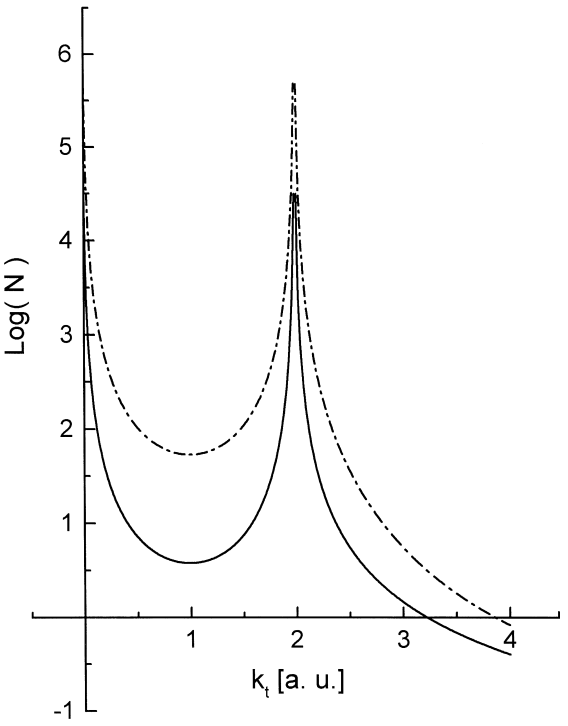

Fig. 1. Square modulus of N_{C3} and N as a function of k_t for $K_t = 2$ (a.u.), $Z_t = Z_p = 1$ and $Z_e = -1$. Solid line, N approx.; dashed line, N_{C3}.

electron in the field of two protons. Fig. 2a–d show that when m increases the particle distribution moves away from the direction where asymptotically the particles move, and on the other hand, the amplitude as a whole decreases. It could be noted that the correlation introduced by the Φ_2 model is determined by the interference given by the cross products, when Eq. (10) is squared. In Fig. 3 we see a contour plot of the interference between the terms $m = 0$ and $m = 1$ in the $\mathbf{r}_t$-plane, the values of charges and momenta are those of Fig. 2. The particle Z_t is in the origin of the coordinates and the vector $\mathbf{r}_p$ was written in terms of $\mathbf{r}_t$ and $\mathbf{R}_t$ with $R_t = 6$ a.u. In the asymptotic region Ω_0, the correlation introduced by the Φ_2 model is of order $O(1/r_t, 1/R_t)$.

The behavior of the wave function in the threshold regions determines the double differential cross sections (DDCS's) around of the SE and ECC cusps for an ionizing collision process. For example, when $k_p \to 0$

$$\Psi_{\Phi_2}(\mathbf{r}_t, \mathbf{R}_t) = N \exp(\mathrm{i}\mathbf{K}_t \cdot \mathbf{R}_t) \times \sum_{m=0}^{\infty} \frac{(-\mathrm{i}\alpha_t)_m}{m!(m)_m} J_{2m}\left[2\sqrt{Z_p Z_e \xi_p}\right] \times F_t[m, \xi_t], \tag{15}$$

where $J_m[z]$ is the Bessel function [18]. Correlation is introduced by orders with $m \neq 0$. The shape of the ECC peak is determined by the successive Bessel functions.

3. DDCS in the Φ_2 approximation

In this section we introduce two different approximations to calculate transition matrices and DDCS's within the Φ_2 framework. In Fig. 2 we observe that the expansion (10) is strongly convergent. This expansion allows us to obtain analytical expressions for the transition matrices in different approximations. We consider that the energy of the incident particle is high enough so that the heavy projectile follows a straight trajectory. In this case, using the impact parameter treatment, the internuclear potential and the wave function for the relative motion of the heavy particles do not contribute to double differential cross sections (differential in the electron velocity) [23]. Then, a general transition matrix in the prior form in a Φ_2 approximation is

$$T = \left\langle \Psi_f^{\Phi_2} | V_i | \Psi_i \right\rangle,$$

where V_i is the perturbation potential acting on the initial state Ψ_i. From Eq. (10), the state $|\Psi_f^{\Phi_2}\rangle$ can be written as

$$\left|\Psi_f^{\Phi_2}\right\rangle = N \sum_m a_m \left|\chi_p^m\right\rangle |\chi_t^m\rangle, \tag{16}$$

with

$$\left\langle \mathbf{r}_j | \chi_j^m \right\rangle = \varphi_{\mathbf{q}_j}(\mathbf{r}_j) F_j[m, \xi_j], \tag{17}$$

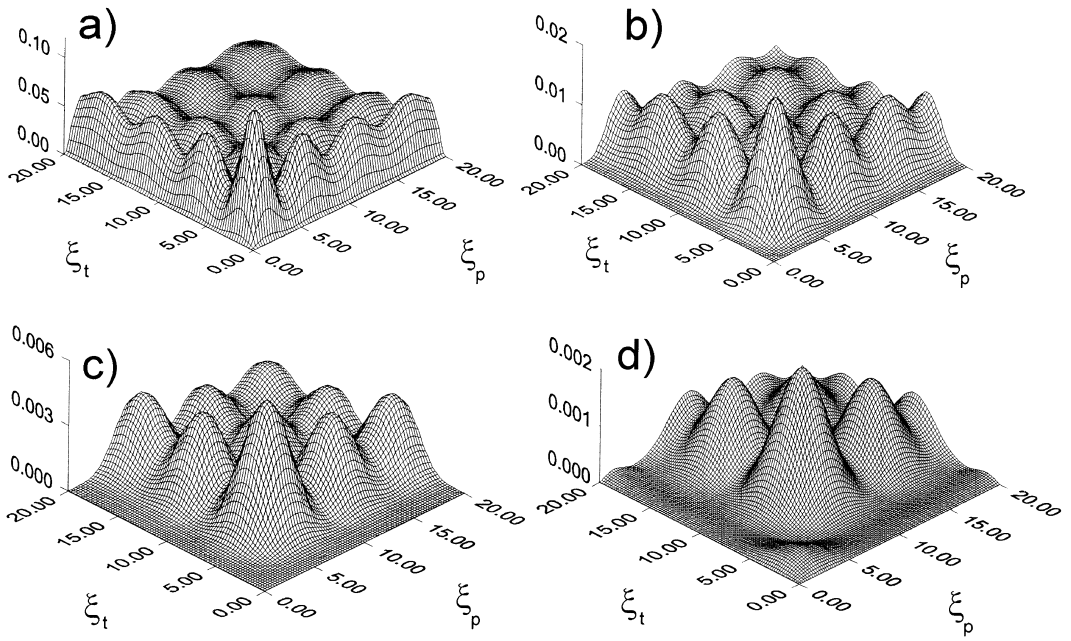

Fig. 2. Particle distribution of an electron in the field of two protons. (a)–(d) show the terms of the series $m = 1$, 2, 3 and 4 in parabolic coordinates ξ_t and ξ_p and $k_t = k_p = 1$ (a.u.).

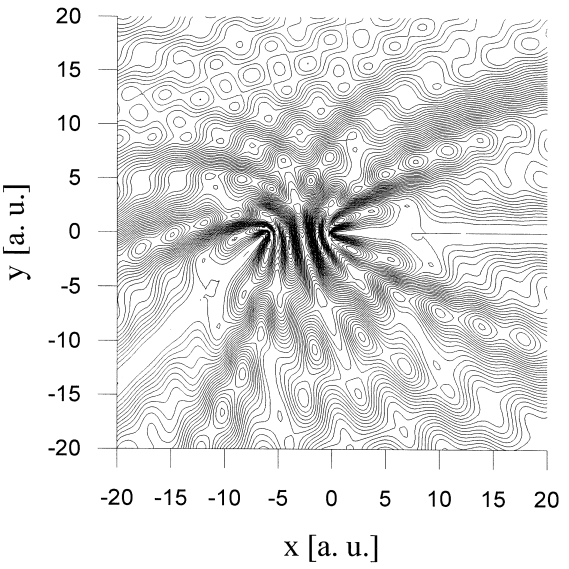

Fig. 3. Contour plot of the interference between the terms $m = 0$ and $m = 1$ in terms of the Cartesian coordinates of the vector $\mathbf{r}_t$. The charges and momenta are equal to those used in Fig. 2. The origin of the coordinates is over the particle Z_t and $R_t = 6$ (a.u.).

where $\varphi_{\mathbf{k}}(\mathbf{r})$ represents the plane wave exp [i$\mathbf{k} \cdot \mathbf{r}$], $\mathbf{q}_t = \mathbf{k}_t + \mathbf{K}_f$ and $\mathbf{q}_p = -\mathbf{K}_f$. The transition matrix reads

$$T^{\Phi_2} = N \sum_m a_m T_m, \qquad T_m = \left\langle \chi_p^m \chi_t^m | V_i | \Psi_i \right\rangle. \tag{18}$$

In this way, the partial matrices T_m resemble the familiar expressions that appear in the calculation of DDCS's in ionization theory. It is clear that different approximations will correspond to different choices of the initial state and its resulting perturbation. The present approach to the transition matrix enables us to test a large variety of generalized multivariable hypergeometric functions for the final state, that differ in the set of coefficients $\{a_m\}$.

A first test of the multivariable continuum wave function is built upon the Born Approximation [23]. This is the case of the so-called Born-Φ_2 approximation (thereafter B-Φ_2), where the function Ψ_i^{B} is the undistorted initial state of the electron in a hydrogenic atom

$$\left\langle \mathbf{R}_t \mathbf{r}_t | \Psi_i^{\mathrm{B}} \right\rangle = \varphi_{\mathbf{K}_i}(\mathbf{R}_t)\psi_i(\mathbf{r}_t) = \varphi_{\mathbf{K}_i}(\mathbf{r}_t)\varphi_{-\mathbf{K}_i}(\mathbf{r}_p)\psi_i(\mathbf{r}_t),$$

and we have considered $m_p, m_t \gg m_e$, the electron mass. The perturbing potential is simply $V_i^B(r_p) = -Z_p/r_p$ and $\psi_i(\mathbf{r}_t)$ represents an hydrogenic ground state. The partial transition matrices are Nordsieck-like integrals, where the second parameter of the hypergeometric functions $F[m, \xi_j]$ is an integer number $1 + 2m$ [24]. Then, T_m splits in target centered times projectile centered partial transition matrices, $T_m = \tilde{T}_p^m \tilde{T}_t^m$. The final expressions are not shown here for brevity [25]. Except for a normalization factor, the first order $m = 0$ in the series representation (Eq. 18) is the commonly known Born-C2 approximation, where the final state of the electron is represented by a C3 wave function and the internuclear interaction is removed by an impact parameter approximation. Then, the C3 function reduces to the product of two outgoing Coulomb wave functions (C2 wave function) and $T^{B-C2} = N_t N_p T_p^0 T_t^0$ where N_l are the normalization factors. Furthermore, by setting $a_p = 0$ and $m = 0$ we recover the well known First Born Approximation [26], i.e. $T^{FBA} = N_t T_p^0(a_p = 0)\, T_t^0$.

A more advanced approximation includes an asymptotically distorted initial state, giving rise to the EIS-Φ_2 (or CCW–EIS, Continuum Correlated Wave–Eikonal Initial State) model

$$\langle \mathbf{r}_t \mathbf{r}_p | \Psi_i^{EIS} \rangle = \varphi_{\mathbf{K}_i}(\mathbf{R}_t)\psi_i(\mathbf{r}_t)\mathscr{E}_{\mathbf{v}_i}(\mathbf{r}_p),$$

where $\mathscr{E}_{\mathbf{k}}(\mathbf{r}) = \exp(i\alpha_i \ln k\eta)$ is the eikonal wave function for the electron–projectile interaction, $\alpha_i = Z_p/v_i$ is the initial channel Sommerfeld parameter, and the perturbation potential reads

$$V_i^{EIS} = -\frac{\nabla_{\mathbf{r}_p}^2}{2\mu_p} + \frac{1}{m_e}\nabla_{\mathbf{r}_p} \cdot \nabla_{\mathbf{r}_t}.$$

The transition matrix is expressed in the same way as Eq. (18), but since now the perturbation potential is a sum of two terms, we have

$$T_m = \left\langle \chi_p^m \chi_t^m \middle| V_i^{EIS} \middle| \Psi_i^{EIS} \right\rangle = I_m + J_m, \tag{19}$$

where $I_m = I_m^p I_m^t$ and $J_m = \mathbf{J}_m^p \cdot \mathbf{J}_m^t$. The situation is not as simple as in the B-Φ_2 approximation, because now the partial transition matrices are given in terms of the two-variable F_1 hypergeometric functions and its derivatives [19]. We note that when $m = 0$ these expressions reduce to the usual CDW–EIS approximation in prior form [27]. We have developed a code to compute the transition matrices in this approximation, but calculation of DDCS is extremely expensive in computing time. Here we restrict our attention to the Born-like theories, that give a rough estimation of the influence of the Φ_2 function. The evaluation of T_p^m and T_t^m involves the computation of derivatives, that has been carried out by a recursive routine that implements the properties of products and composition of derivatives [28]. As we have pointed out before, the series that represents the transition matrix inherits a strong numerical convergence of Eq. (10), for this reason it is necessary to sum only few terms of the series (commonly no more than five), that is to say

$$T^{\Phi_2} \approx T_M^{\Phi_2} = N \sum_{m=0}^{M} a_m T_m. \tag{20}$$

The DDCS in the electron energy and emission angle is defined as

$$\sigma(E, \Omega) = \frac{d^2\sigma}{dE\, d\Omega} = (2\pi)^4 v_i \frac{k_t}{K_i} \int |T|^2 \, d\Omega_p,$$

where the integration is carried out over the angular degrees of freedom Ω_p of the projectile. We introduce the symbol

$$\sigma_M(E, \Omega) = (2\pi)^4 v_i \frac{k_t}{K_i} \int \left|T_M^{\Phi_2}\right|^2 d\Omega_p, \tag{21}$$

and $\sigma(E, \Omega) = \sigma_{M\to\infty}(E, \Omega)$. We verify that a sum up to $M = 4$ of the series enables us to obtain the DDCS with a 1% relative error. Furthermore, the main correction to the order $m = 0$ is provided by the first one, and then the first partial sum $\sigma_{M=1}$ gives a rough idea of the full DDCS.

Now, we test the B-Φ_2 approximation for helium targets. We consider the target in the ground state represented by a one electron model with a five term Roothan–Hartree–Fock orbital [29]. The state of the electron in the final channel is modelled by a Φ_2 continuum wave function with effective charge of $Z_t = 1.6875$. We should point out that this is a rough approximate way to include the effect of the passive electron of helium in the final

state, however, a Φ_2-correlated final state with passive electrons is not available at the moment.

In Fig. 4 we compare the theoretical DDCS in the forward direction for the collision $H^+ + He \rightarrow H^+ + He^+ + e^-$ with the experimental data of Lee et al. [30]. The impact energy of the collision is 1.5 MeV/amu. We plot the results of undistorted calculations (FBA, B-C2 and B-Φ_2) and the CDW–EIS calculations. The B-Φ_2 theory qualitatively agrees with the experimental data, giving all the main features of the forward ejected electrons. The projectile distortion in the final channel gives the ECC cusp for the B-C2 and the B-Φ_2 approximations, even when the initial state is undistorted. The B-Φ_2 approximation gives an asymmetric ECC peak, i.e. an enhancement of the electronic emission for velocities lower than the projectile one, but the B-C2 and CDW–EIS models fail to reproduce this feature. That asymmetry is mainly given by the interference between the zero and the first terms in Eq. (20). The B-Φ_2 approximation gives a good agreement with experimental data in the region of the ridge electrons, but the agreement becomes worse in the soft electron region overestimating the SE asymmetry. The Φ_2 final wave function is correlated and therefore an equivalent correlated initial channel should be considered instead the simple Born one. Such initial state is under study.

A similar picture for 100 keV collisions is shown in Fig. 5 where the experimental data were obtained by Bernardi et al. [31]. In this case, the agreement of the B-Φ_2 approximation is good in the ridge region, while all theories fail in the binary sphere. Here again the enhancement of the emission of ridge electrons over the CDW–EIS theory is mainly driven by the introduction of a correlated final state. The B-C2 model also correctly describes the ridge region, but overestimates the DDCS's for electrons faster than the projectile velocity. As in the previous case, the B-Φ_2 model is the only one that accounts for the asymmetry of the ECC peak.

Now we can turn the attention to the angular structure of the DDCS. In Fig. 6 we plot the DDCS as a function of the emission angle for 300 keV protons colliding with helium. The energies considered for the emitted electrons correspond to velocities near the SE peak ($v \sim 0$), near the ECC peak ($v \sim v_p$) and in the binary sphere ($v \sim 2v_p$). Experimental data are from Rudd et. al. [32]. It can be seen that there is a general agreement with the data. In the low electron energy region, the B-Φ_2 theory underestimates the data for large angles, giving rise to an angular asymmetry in the SE peak higher than expected. The dynamical correlation

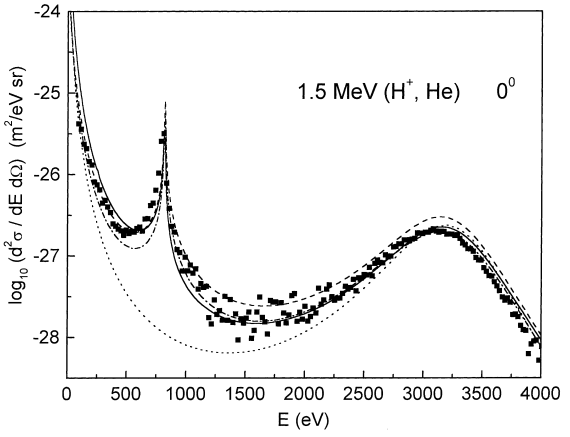

Fig. 4. DDCS at 0 degree for a 1.5 MeV (H^+,He) collision. Solid line, Born-Φ_2 approx.; dashed line, B-C2; dotted line, FBA; dash-dotted line, CDW–EIS. The experimental data are from Ref. [30]. From Ref. [25].

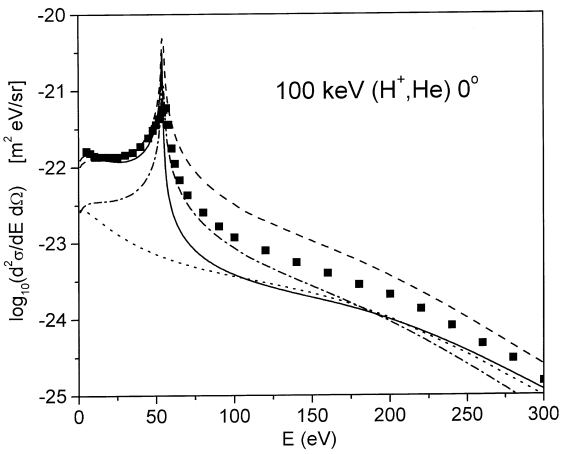

Fig. 5. Same as Fig. 4 but for 100 keV (H^+,He) collision. The experimental data are from Ref. [31].

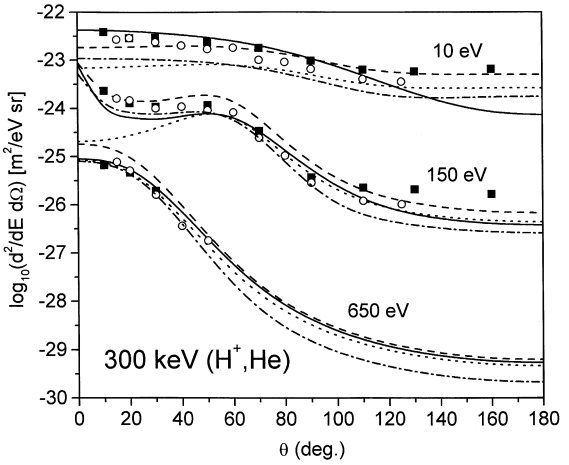

Fig. 6. Angular distribution of ejected electrons for a 300 keV (H^+,He) collision. Energies correspond to soft electrons (10 eV), ECC electrons (150 eV) and binary electrons (650 eV). The experimental data were obtained by Rudd et al. [32]. For the notations of theories see caption of Fig. 4.

introduced by the Φ_2 wave function in the final state seems to give the electron–projectile interaction effects required to produce asymmetric SE and ECC cusps.

4. Discussion and outlook

In this work we have presented a correlated model for ionizing ion–atom collisions. This model is based on a set of new approximative solutions for the final channel of the process represented by a three-body continuum Coulomb system. These new solutions can be written as multivariable hypergeometric functions that fully correlate the motion of the electron relative to the heavy ions. We propose a final state which results from the simplest mathematical approximation to the non-diagonal kinetic energy. This leads us to the Φ_2 wave function. A more elaborate approximation requires the development of more sophisticated hypergeometric functions that are not available at the moment.

In the second section of this work we have shown the fundamental characteristics of the Φ_2 wave function. The Φ_2 function exhibits a high probability to find the electron in the spatial region comprised between the two heavy centers (Fig. 3). The normalization factor mixes in a non-separable way the Sommerfeld parameters related with the electron–projectile and electron–target interactions, giving rise to the SE and ECC peaks. We have shown that the C3 approach is a first order in the series expansion in terms of two-dimensional harmonic oscillators. The interference between the terms of this series introduces the asymmetry in the peaks and increases the yield of ridge electrons in an appropriate way. In this context we note that a cusp of opposite asymmetry was observed recently for the collisional double electron detachment from H^- [34]. In this case the outgoing charged particles are two electrons and one proton. Recently the authors and co-workers have presented a wave function for such a system based on multivariable hypergeometric functions [35]. We hope that this kind of function may reproduce the unusual asymmetry of the cusp observed in the double electron detachment experiment.

The relative motion of the heavy particles remains described by a Coulomb function. The corresponding normalization factor produces an exaggerated decrement of cross sections for decreasing ion impact energy. This indicates that also this motion should be correlated. This can be done by introducing additional terms of the non diagonal kinetic energy and obtaining a system of three coupled differential equations. It is possible to introduce a multivariable hypergeometric Φ_3 which correlate all the variables, with poorly known mathematical properties.

We have obtained DDCS's for the collision of protons with helium targets in Born-Φ_2 approximation. The theory well describes all the features of the cross section, but exaggerates the asymmetry of the SE emission. A possible solution to these disagreements could be the introduction of the electron-projectile interaction in the initial channel. Furthermore, a correlated initial state derived within the Φ_2 approach would be more adequate, since in that case both functions would be solutions of the same Hamiltonian and thus orthogonal.

Finally, we would like to note that the description of the final interaction between the

electron and the residual He^+ target has been modelled by an effective charge. It has been shown that the effect of the passive electrons should be taken into account in a more accurate way than this simple model [27,33]. A suitable extension of the theory should include this effect in the calculation of the final state wave function through the introduction of model potentials.

Acknowledgements

We would like to acknowledge J.E. Miraglia, P. Macri and W.R. Cravero for fruitful discussions.

References

[1] R.Moshammer et al., Phys. Rev. Lett. 73 (1994) 3371.
[2] N. Stolterfoht, R.D. DuBois, R.D. Rivarola, Electron emission in Heavy Ion–Atom Collisions, Springer, Berlin, 1997.
[3] C.R. Garibotti, J.E. Miraglia, Phys. Rev. A 21 (1980) 572.
[4] Dz. Belkič, J. Phys. B 11 (1978) 3529.
[5] D.S.F. Crothers, J.F.J. McCann, J. Phys. B 16 (1983) 3229.
[6] P.D. Fainstein, V.H. Ponce, R.D. Rivarola, J. Phys. B 24 (1991) 3091.
[7] J.E. Miraglia, J. Macek, Phys. Rev. A 43 (1991) 5919.
[8] E.A. Alt, A.M. Mukhamedzhanov, Phys. Rev. A 47 (1993) 2004.
[9] Y.E. Kim, A.L. Zubarev, Phys. Rev. A 56 (1997) 521.
[10] F.D. Colavecchia, G. Gasaneo, C.R. Garibotti, Phys. Rev. A 57 (1998) 1018.
[11] Sh.D. Kunikeev, J. Phys. B: At. Mol. Opt. Phys. 31 (1998) 2649.
[12] A. Erdelyi, Proc. Roy. Soc. of Edinburg LIX (1938-39) 224.
[13] A. Erdelyi, Proc. Roy. Soc. of Edinburg LX (1939-40) 344.
[14] H. Klar, Z. Phys. D 16 (1990) 231.
[15] D.S.F. Crothers, L.J. Dubé, Advances in Atomic, Molecular and Optical Physics, vol. 30, 1993.
[16] G. Gasaneo, F.D. Colavecchia, C.R. Garibotti, J.E. Miraglia, P. Macri, Phys. Rev. A 55 (1997) 2809.
[17] G. Gasaneo, F.D. Colavecchia, C.R. Garibotti, J.E. Miraglia, P. Macri, J. Phys. B 30 (1997) 265.
[18] M. Abramowitz, I.A. Stegun, Handbook of Mathematical Functions, Dover Publications, New York, 1970.
[19] P. Appell, J. Kampé de Feriet, Fonctions Hypergéométriques et Hypersphériques; Polynômes Polynômes d'Hermite, Gauthier–Villars, Paris, 1926.
[20] P.J. Redmond (unpublished); L. Rosenberg, Phys. Rev. D 8 (1973) 1833.
[21] J.L. Burchnall, T.W. Chaundy, J. Math. 12 (1941) 112.
[22] G. Gasaneo, PhD thesis, Instituto Balseiro, 1998.
[23] M.R.C. McDowell, J.P Coleman, Introduction to the theory of ion–atom collisions, North-Holland, Amsterdam, 1970.
[24] F.D. Colavecchia, G. Gasaneo, C.R. Garibotti, J. Math. Phys. 38 (1997) 6603.
[25] F.D. Colavecchia, G. Gasaneo, C.R. Garibotti, accepted for publication in Phys. Rev. A.
[26] H. Bethe, Ann. Phys. 5 (1930) 325.
[27] W. Cravero, PhD thesis, Instituto Balseiro, 1997.
[28] I.S. Gradshteyn, I.M. Ryzhik, Table of Integrals, Series and Products, Academic Press, Orlando, 1980.
[29] C. Clemente, C. Roetti, At. Data Nucl. Data Tables 14 (1974) 445.
[30] D.H. Lee, P. Richard, T.J.M. Zouros, J.M. Sanders, J.L. Shinpaugh, H. Hidmi, Phys. Rev. A 41 (1990) 4816.
[31] G. Bernardi, S. Suárez, P. Fainstein, C.R. Garibotti, W. Meckbach, P. Föcke, Phys. Rev. A 40 (1989) 6863.
[32] M.E. Rudd, L.H. Toburen, N. Stolterfoht, At. Data. Nucl. Data Tables 18 (1976) 413.
[33] L. Gulyás, P.D. Fainstein, A. Salin, J. Phys. B: At. Mol. Opt. Phys 28 (1995) 245.
[34] L. Víkor, L. Sarkadi, F. Penent, A. Báder, J. Pálinkás, Phys. Rev. A 54 (1996) 2161.
[35] P. Macri, J.E. Miraglia, F.D. Colavecchia, C.R. Garibotti, G. Gasaneo, Phys. Rev. A 55 (1997) 3518.